Motor protein mutations cause a new form of hereditary spastic paraplegia

Andrés Caballero Oteyza, MSc
Esra Battaloğlu, PhD
Levent Ocek, MD
Tobias Lindig, MD
Jennifer Reichbauer, BSc
Adriana P. Rebelo, PhD
Michael A. Gonzalez, MSc
Yasar Zorlu, MD
Burcak Ozes, MSc
Dagmar Timmann, MD
Benjamin Bender, MD
Günther Woehlke, PhD
Stephan Züchner, MD, PhD
Ludger Schöls, MD
Rebecca Schüle, MD

Correspondence to Dr. Schüle: r.schule@med.miami.edu

ABSTRACT

Objective: To identify a novel disease gene in 2 families with autosomal recessive hereditary spastic paraplegia (HSP).

Methods: We used whole-exome sequencing to identify the underlying genetic disease cause in 2 families with apparently autosomal recessive spastic paraplegia. Endogenous expression as well as subcellular localization of wild-type and mutant protein were studied to support the pathogenicity of the identified mutations.

Results: In 2 families, we identified compound heterozygous or homozygous mutations in the kinesin gene *KIF1C* to cause hereditary spastic paraplegia type 58 (SPG58). SPG58 can be complicated by cervical dystonia and cerebellar ataxia. The same mutations in a heterozygous state result in a mild or subclinical phenotype. *KIF1C* mutations in SPG58 affect the domains involved in adenosine triphosphate hydrolysis and microtubule binding, key functions for this microtubule-based motor protein.

Conclusions: *KIF1C* is the third kinesin gene involved in the pathogenesis of HSPs and is characterized by a mild dominant and a more severe recessive disease phenotype. The identification of *KIF1C* as an HSP disease gene further supports the key role of intracellular trafficking processes in the pathogenesis of hereditary axonopathies. ***Neurology*® 2014;82:2007–2016**

GLOSSARY

ATP = adenosine triphosphate; **BICDR-1** = bicaudal-D-related protein 1; **DMEM** = Dulbecco's modified Eagle medium; **FCS** = fetal calf serum; **HSP** = hereditary spastic paraplegia; ***HSP60*** = heat shock 60kDa protein 1; ***KIF1C*** = kinesin family member 1C; **p-loop** = phosphate-binding loop; **SPG58** = hereditary spastic paraplegia type 58; **WB** = Western blot; **WES** = whole-exome sequencing.

Hereditary spastic paraplegias (HSPs) are among the most heterogeneous mendelian diseases.[1] The pathologic hallmark of HSPs is a length-dependent distal axonopathy of the upper motor neurons. To maintain their high degree of polarization, corticospinal tract motor neurons critically depend on efficient mechanisms to selectively distribute proteins and membrane components throughout the cell. It is therefore not surprising that a large number of HSP proteins interfere with membrane trafficking pathways in various ways: by affecting membrane curvature and/or the morphology of the endoplasmic reticulum (Reep1, RTN2, spastin, atlastin-1), by modifying vesicle sorting and trafficking along the secretory or endosomal pathway (adapter protein complexes, strumpellin, vcp, vps37a), or by disturbing axonal transport (KIF5A, spastin) (reviewed in reference 2).

In this study, we used whole-exome sequencing (WES) to identify the genetic cause of a novel form of complicated HSP, termed hereditary spastic paraplegia type 58 (SPG58).

METHODS

Exome sequencing. WES was performed on the index patients of families THI26001 (P3) and IHG25215 (P5) (figure 1A). After exome capture via the SureSelect Human All Exon 50 Mb kit (Agilent, Santa Clara, CA), samples were sequenced on HiSeq2000 instruments (Illumina, San Diego, CA). An average of 70,811,663 sequence reads of 100–base pair length were produced per sample, 98.8% of

Supplemental data at Neurology.org

From the Hertie-Institute for Clinical Brain Research (A.C.O., J.R., L.S., R.S.), Department of Neurodegenerative Diseases, University of Tübingen, Germany; Bogazici University (E.B., B.O.), Department of Molecular Biology and Genetics, Istanbul; Tepecik Research and Training Hospital (L.O., Y.Z.), Clinics of Neurology, Izmir, Turkey; Diagnostic and Interventional Neuroradiology (T.L., B.B.), Department of Radiology, University Hospital Tübingen; German Research Center for Neurodegenerative Diseases (DZNE) (J.R., R.S., L.S.), Tübingen, Germany; Dr. John T. Macdonald Foundation Department of Human Genetics and John P. Hussman Institute for Human Genomics (A.P.R., M.A.G., S.Z., R.S.), University of Miami Miller School of Medicine, FL; Department of Neurology (D.T.), University of Duisburg-Essen; and Department of Physics E22 (Biophysics) (G.W.), Technical University Munich, Garching, Germany.

Go to Neurology.org for full disclosures. Funding information and disclosures deemed relevant by the authors, if any, are provided at the end of the article.

Figure 1 Pedigrees and mutations in the *KIF1C* gene

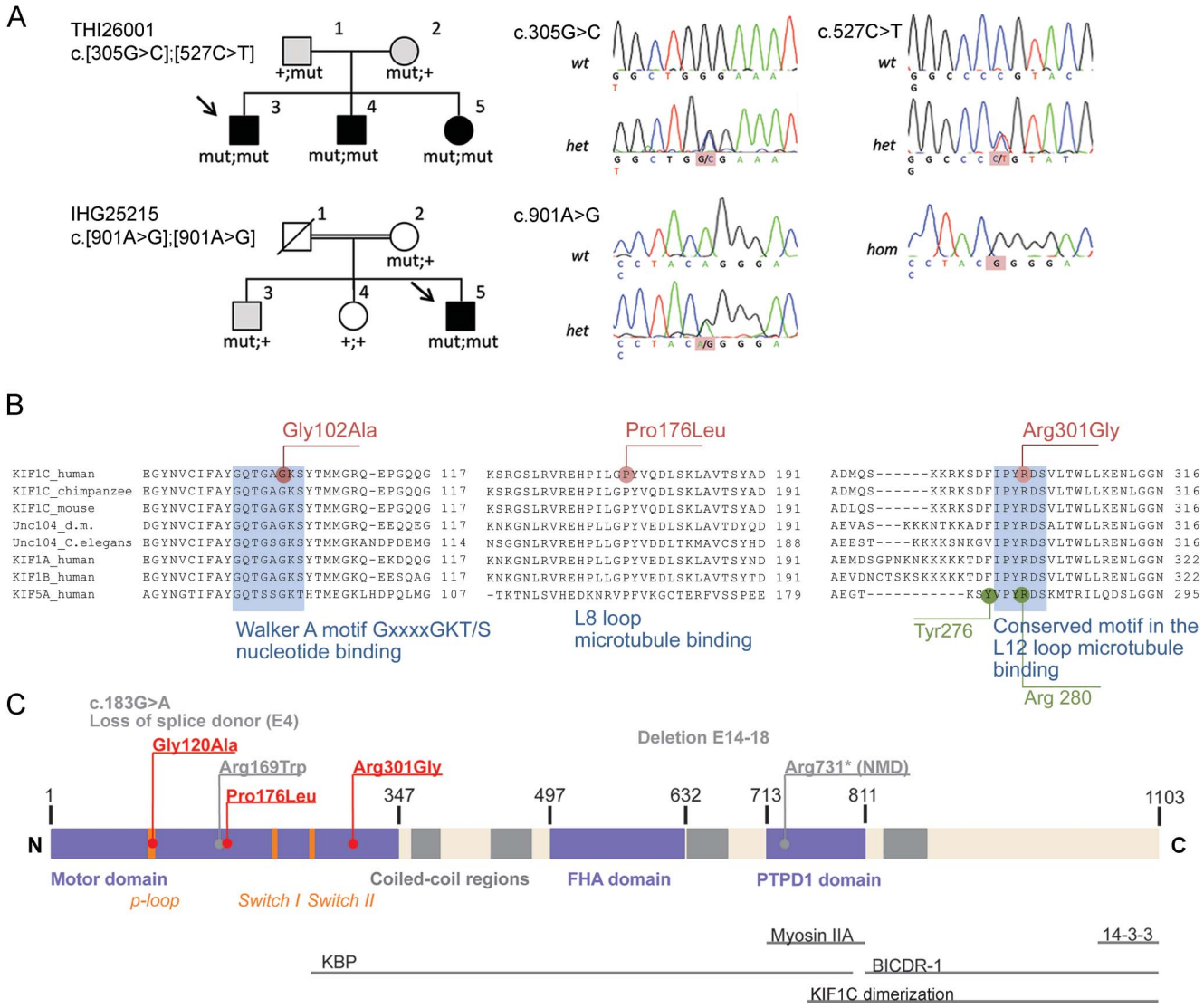

(A) The *KIF1C* variants c.[305G>C];[527C>T], p.[Gly102Ala];[Pro176Leu], and c.[901A>G];[901A>G], p.[Arg301Gly];[Arg301Gly] segregate in families THI26001 and IHG25215, respectively. Severely affected family members are depicted by black boxes and are homozygous or compound heterozygous for the respective mutations. Mildly or subclinically affected family members are depicted by gray boxes and are carriers of one mutant allele each. Electropherograms are shown on the right. (B) All 3 *KIF1C* mutations (red) affect amino acids that are highly conserved across species as well as among kinesin-3 and -1 families. Gly102Ala is located within the Walker A motif (GxxxxGKT/S) of the so called p-loop, essential for nucleotide binding, and therefore likely renders KIF1C catalytically inactive. Both Pro176Leu (loop 8) and Arg301Gly (loop 12) affect the microtubule binding interface of KIF1C. *KIF5A* mutations causing autosomal dominant SPG10 are shown in green. The uniprot alignment tool was used to generate alignments with the following protein identifiers: KIF1C_human: O43896; KIF1C_chimpanzee: K7BP32; KIF1C_mouse: O35071; unc104_d.m.: A1ZAJ2; unc104_*C elegans*: P23678; KIF1A_human: Q12756; KIF1B_human: O60333; and KIF5A_human: Q12840. (C) Domain structure of the *KIF1C* gene. Known interaction partners and putative binding regions of *KIF1C* are depicted by horizontal lines. Mutations detected in this study are indicated in red, mutations published by Dor et al.[26] in gray.

which could be aligned to the target sequence. Mean coverage was 57-fold. Data were analyzed using the browser interface of the Genomes Management Application GEM.app.[3] Candidate variants were confirmed with conventional Sanger sequencing.

Cell culture. Fibroblast lines were established from skin biopsies using standard procedures. Cells were grown in Dulbecco's modified Eagle medium (DMEM) plus 10% fetal calf serum (FCS) and maintained at 37°C and 5% CO_2. Lymphocytes were isolated from blood samples and immortalized by exposure to Epstein-Barr virus. Cells were cultivated in Roswell Park Memorial Institute medium plus 20% FCS and maintained at 37°C and 5% CO_2. The motor neuron–like hybrid cell line NSC-34 and the fibroblast-like cell line COS-7 were cultured in DMEM plus 10% FCS at 37°C, 5% CO_2.

Quantitative PCR. RNA was extracted and transcribed using standard protocols. Control fibroblasts and lymphoblasts were matched to patient cells for age (±5 years), sex, and cell passage (±2 passages). Quantitative PCR was run on a LightCycler 480 device (Roche Applied Science, Penzberg, Germany).

Western blot. Protein was isolated from primary fibroblast and lymphoblast cell lines using standard protocols. After sodium dodecyl sulfate–polyacrylamide gel electrophoresis, samples were

transferred onto a polyvinylidene difluoride membrane, washed 3 times with 1x Tris-buffered saline/Tween 20, and blocked with 1x Tris-buffered saline/Tween 20 + 5% skimmed milk. The membrane was incubated with the primary antibody overnight in blocking buffer and with the secondary antibody for 1 hour at room temperature. Detection was performed using ECL reagent (Thermo Fisher Scientific, Waltham, MA).

Cloning. The *KIF1C* ORF was amplified from a complementary DNA clone[4] and transferred into a pcDNA3.1/CT-GFP-TOPO expression vector (Invitrogen, Carlsbad, CA). Site-directed mutagenesis was performed on the resulting pTOPO-GFP-KIF1C$_{wt}$, using QuikChange II XL (Agilent), introducing the human mutations c.305G>C (pTOPO-GFP-KIF1C$_{Gly102Ala}$), c.527C>T (pTOPO-GFP-KIF1C$_{Pro176Leu}$), and c.901A>G (pTOPO-GFP-KIF1C$_{Arg301Gly}$). Identity with the reference sequence (NM_006612.5) and introduction of the desired mutations was confirmed by conventional sequencing. Restriction enzyme digest was used to transfer the inserts to pmCherry-N1 (Clontech Laboratories, Mountain View, CA).

Immunofluorescence. Cells were fixed in 4% paraformaldehyde and stained with specific primary antibodies and Alexa-conjugated secondary antibodies. Cells were mounted on coverslips with Prolong Gold Antifading Reagent with DAPI (4',6-diamidino-2-phenylindole) (Invitrogen). Pictures were taken with a Zeiss LSM 710 inverted confocal microscope using the ZEN2010 software (Carl Zeiss Corporation, Oberkochen, Germany). Finally, images were processed with the ImageJ software (http://rsbweb.nih.gov).

Antibodies. The following antibodies were used: rabbit polyclonal anti-KIF1C (AKIN11; Cytoskeleton Inc., Denver, CO), dilution 1:250 (immunofluorescence) and 1:500 (Western blot [WB]); mouse monoclonal anti-α-tubulin (A-11126; Invitrogen), dilution 1:200 (immunofluorescence); mouse monoclonal anti-α-tubulin (T6074; Sigma-Aldrich, St. Louis, MO), dilution 1:5,000 (WB); and mouse anti-GAPDH (glyceraldehyde 3-phosphate dehydrogenase) (clone 6C5; Millipore Corporation, Billerica, MA), dilution 1:5,000 (WB).

Statistics. Statistical analyses were performed using SPSS software version 20 for Mac (IBM Corporation, Armonk, NY). Two-sided *t* tests were used to compare KIF1C levels between groups.

Standard protocol approvals, registrations, and patient consents. Informed consent was obtained from all individuals involved in the study, and the institutional review boards of the participating medical centers approved the study.

RESULTS

Exome sequencing and identification of the *KIF1C* gene (SPG58). We performed WES in the index patient of a German family with apparently autosomal recessive HSP (THI26001, figure 1A) and filtered the resulting variants for allele frequency (EVS6500 <0.5%), genotype frequency in the GEM.app database (number of families with segregating variant ≤10), conservation across species (GERP score >1 or PhastCons score >0.4), effect on protein function (Polyphen-2 score >0.3), and quality (GATK QUAL score >50, genotype quality GQ >50). None of the known HSP genes contained any variants matching the filter criteria. Only 5 potentially novel candidate genes remained on the hit list, containing either 2 heterozygous (n = 4) or 1 homozygous (n = 1) variant: *KIF1C*, *LYST*, *TENM1*, *SAMD11*, and *OVOS*. To narrow down this candidate gene list, we analyzed all variants for cosegregation with the disease. Only the 2 variants in the *KIF1C* gene (NM_006612.5) cosegregated completely: c.[305G>C];[527C>T], p.[Gly102Ala];[Pro176Leu] (figure 1A, table e-1 on the *Neurology*® Web site at Neurology.org).

To further support the role of *KIF1C* as a disease gene, we revisited the exomes of 186 index patients with genetically unresolved HSP (n = 126), ataxia (n = 30), or spastic ataxia (n = 30) compatible with autosomal recessive modes of inheritance. One additional family (IHG25215) carried a highly conserved unknown homozygous *KIF1C* variant: c.[901A>G];[901A>G], p.[Arg301Gly];[Arg301Gly]. This variant cosegregated with disease (figure 1A).

Clinical description of SPG58 families. *THI26001.* All 3 affected siblings presented with adult-onset (18–30 years) spastic ataxia with predominant lower limb spasticity and weakness. Cerebellar ataxia was present in all 3 with cerebellar oculomotor disturbance (2/3) and upper > lower limb ataxia (3/3). Dorsal column sensory deficits (3/3) were rather pronounced compared with most other HSP subtypes. Although not formally tested, none of the family members showed an indication of cognitive involvement. Details on the phenotype are given in table 1.

Neurophysiologic studies indicated a widespread demyelinating process with central and peripheral involvement. Motor evoked potentials showed increased central motor conduction times at early disease stages and were later absent when recorded from the upper and the lower limbs. The long sensory tracts were similarly involved with prolonged or absent cortical potentials. Increased latencies were also observed for visual (2/3) and auditory (1/3) evoked potentials. One sibling showed peripheral involvement with a demyelinating sensory-motor peripheral neuropathy.

MRIs revealed signs of widespread T2 hyperintensities primarily affecting the pre- and postcentral white matter, pyramidal tracts, superior cerebellar peduncles, and the occipital white matter with relative sparing of the optic radiations (figure 2).

Both parents are carriers of one of the *KIF1C* mutations. The father had consulted a neurologist a few weeks prior because of a subjective limping and some sensory deficits in his legs. The mother reported no gait problems. Closer clinical examination revealed a carrier phenotype in both of them, consisting of lower limb weakness with central distribution (proximal > distal, hip abductors > hip adductors) and demyelinating sensory-motor neuropathy in the father (Gly102Ala) and mild signs of pyramidal involvement (brisk reflexes, extensor plantar response) in the mother (Pro176Leu). The MRIs of both parents also showed T2

Table 1 Phenotypes and characteristics of the families

	THI26001-3	THI26001-4	THI26001-5	THI26001-1	THI26001-2	IHG25125-5	IHG25125-3
Origin	Germany	Germany	Germany	Germany	Germany	Turkey	Turkey
Sex	Male	Male	Female	Male	Female	Male	Male
Genotype	Gly102Ala/Pro176Leu	Gly102Ala/ Pro176Leu	Gly102Ala/Pro176Leu	Gly102Ala/wt	Wt/Pro176leu	Arg301Gly/ Arg301Gly	Arg301Gly/wt
Age at onset, y	18	30	18	69	NA	10	16
Age at last examination, y	48	45	42	69	67	48	46
Severity SPRS	30	26	27	7	3	ND	ND
UL							
Spasticity	–	–	+	–	–	–	–
Reflexes	Normal	Normal	Increased	Decreased	Increased	Normal	
Weakness	–	–	–	–	–	–	–
Amyotrophy	–	–	–	–	–	–	–
LL							
Spasticity	+++	++	+++	-	-	+++	++
Reflexes	Increased	Increased	Increased	Normal	Increased	Increased	Increased
Weakness	+ (distal predominant)	+	++ (distal predominant)	+ (proximal predominant)	–	++ (distal predominant)	+ (distal predominant)
Amyotrophy	–	–	–	–	–	–	–
Extensor plantar sign	+	+	+	–	+	+	+
Cognition	Normal	Normal	Normal	Normal	Normal	Normal	Normal
Oculomotor disturbance	Upward vertical gaze palsy	Cerebellar (saccadic pursuit, gaze-evoked nystagmus)	Cerebellar (saccadic pursuit, gaze-evoked nystagmus, dysmetric saccades)	–	–	–	–
Cerebellar ataxia	UL > LL limb ataxia, UL intention tremor	UL > LL limb ataxia, UL intention tremor	UL > LL limb ataxia, UL intention tremor	–	–	–	–
Dysarthria	Mild	Mild	Moderate			Mild	–
Dystonia	–	–	Mild cervical dystonia	–	–	–	–
Vibration sense	LL distal absent	LL distal reduced	LL distal reduced	LL distal reduced	LL distal absent	LL distal absent	LL distal absent
Urinary symptoms	–	–	–	–	–	–	–
Other symptoms	Irregular head tremor	–	–	–	–	–	–
Nerve conduction studies	Normal	Demyelinating sensory-motor neuropathy	Normal	Demyelinating sensory-motor neuropathy	ND	ND	Sensory-motor neuropathy
Evoked potentials	VEP: increased latency; AEP: normal; MEP: not possible because of head tremor; Tib-SEP: no cortical potential	VEP: increased latency; AEP: increased latency over brainstem; MEP: UL/LL no potential; Tib-SEP: no cortical potential	VEP: normal; AEP: normal; MEP: UL/LL no potential (at age 34 prolonged CMCT); Tib-SEP: increased latency cortical potential	ND	ND	ND	VEP: normal; AEP: normal; MEP: ND; Tib-SEP: no cortical potential
Imaging	MRI: T2 hyperintensities (pre-/postcentral/occipital white matter, pyramidal tract, superior cerebellar peduncles), mild global cerebral atrophy, pronounced tegmental and vermian cerebellar atrophy	ND	MRI: T2 hyperintensities (pre-/postcentral/ occipital white matter, pyramidal tract, superior cerebellar peduncles), mild vermian cerebellar and spinal atrophy	MRI: mild T2 hyperintensities (pyramidal tract, optic radiation), mild cerebellar atrophy	MRI: mild T2 hyperintensities (pyramidal tract, superior cerebellar peduncles)	ND	MRI: mild T2 hyperintensities (pyramidal tract)

Abbreviations: AEP = auditory evoked potentials; CMCT = central motor conduction time; LL = lower limbs; MEP = motor evoked potentials; ND = not done; Tib-SEP = tibial sensory evoked potentials; SPRS = Spastic Paraplegia Rating Scale; UL = upper limbs; VEP = visual evoked potentials; wt = wild-type.

Figure 2 Brain MRI of family THI26001

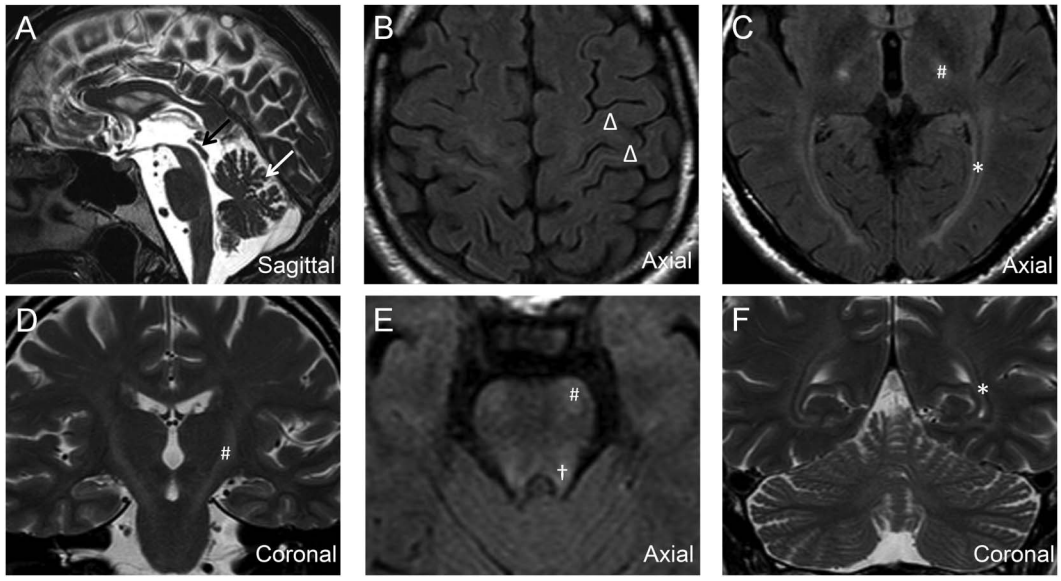

Brain T2-weighted imaging (B, C, E, fluid-attenuated inversion recovery) of THI26001-3 (age 48 years) reveals symmetrical T2-hyperintense cerebral and mild cerebellar demyelination affecting the pre- and postcentral white matter (Δ in B), the pyramidal tracts (# in C–E), the occipital white matter with relative sparing of the optic radiations (* in C and F), and the superior cerebellar peduncles († in E). The midsagittal view (A) shows mild tegmental (black arrow) and vermian cerebellar (white arrow) atrophy.

hyperintensities with a similar pattern, albeit less intense than in the affected offspring (figure e-1).

IHG25215. The 2 affected siblings of consanguineous descent (parents first-degree cousins) of family IHG25215 both reported an unsteady gait since their adolescence, but with different disease course. While the disease progressed insidiously in the younger brother (IHG25215-5), leading to loss of the ability to walk and caregiver dependency in his early 40s, the disease was apparently stable in the older brother (IHG25215-3) who is working full-time and displays only mildly spastic gait not interfering with his daily activities at age 46.

On examination, both brothers exhibited a lower limb spastic paraparesis, mild in IHG25215-3 and severe in IHG25215-5. In the latter, additionally mild cervical dystonia and loss of vibration sense in the lower extremities were noted. The mother of the 2 siblings (IHG25215-2) reported no gait problems at the age of 67 and her neurologic examination was normal. Cognition appeared normal in all family members.

IHG25215-2 and -3 received a neurophysiologic examination. While normal in the mother, the mildly affected sibling showed absence of somatosensory evoked cortical potentials and sensory-motor neuropathy.

Localization of mutations. KIF1C is a kinesin-type microtubule-dependent motor protein that belongs to the kinesin-3 subfamily. It contains an N-terminal conserved kinesin motor domain with several characteristic features: the phosphate-binding loop (p-loop) responsible for adenosine triphosphate (ATP) hydrolysis and propagation of nucleotide-dependent conformational changes from the ATP binding pocket to the microtubule binding region. The latter is often called switch-2 cluster and is formed by helix α4, loop L12, helix α5, and supporting structures[5] (figure 1C). In addition, members of the kinesin-3 subfamily contain a stretch of positively charged lysine residues thought to enhance microtubule binding[6] (k-loop). The SPG58 mutations are found in the p-loop and the switch-2 cluster.

Gly102 is located within the highly conserved Walker A motif of the nucleotide binding p-loop. Mutation of this glycine residue to alanine presumably renders KIF1C catalytically inactive, as noted for the neighboring Lys103Ala mutation.[7] The mutant may no longer be capable of binding nucleotide, and is possibly less stable (see below).

Pro176 is part of loop 8 of the kinesin's motor domain and thus close to the microtubule interaction domain. Functional studies are lacking. Arg301 lies at the core of a highly conserved motif in the L12 loop, involved in microtubule interaction. The homologous amino acid in KIF5A (Arg280) is a mutational hotspot in the autosomal dominant HSP subtype SPG10.[8,9] The Arg280Ala mutant has been shown to reduce microtubule affinity in vitro, suggesting impaired transport rates.[10]

Impact of identified mutations on KIF1C expression. To check whether the mutations affect expression levels of

KIF1C, we compared messenger RNA and protein levels between lymphoblasts and fibroblasts of family THI26001 with age- and sex-matched controls. KIF1C messenger RNA levels among those affected, heterozygous carriers, and controls (figure e-2A) were not significantly different applying quantitative real-time PCR to lymphoblasts. In contrast, protein levels of KIF1C in lymphoblasts of affected persons were reduced to 45% in WBs. These results were confirmed in patient-derived fibroblasts, in which KIF1C protein was reduced to a level of 58% (figure e-2, B and C). The polyclonal antibody used is directed against the KIF1C neck domain and does not specifically recognize wild-type or mutant KIF1C. Of note, the heterozygous carrier of the Gly102Ala mutation (father, P1) showed KIF1C protein levels comparable to his affected offspring (P3-5), whereas KIF1C protein levels in the carrier of the Pro176Leu mutation (mother, P2) were comparable to the control probands' levels. This pattern indicates that the Gly102Ala mutation renders the KIF1C protein less stable, leading to significantly reduced protein levels.

Subcellular localization of endogenous KIF1C protein. We have studied the localization of KIF1C in several cell lines, including human primary fibroblasts (data not shown), a fibroblast-like cell line (COS-7), a human

Figure 3 Subcellular localization of endogenous and overexpressed KIF1C

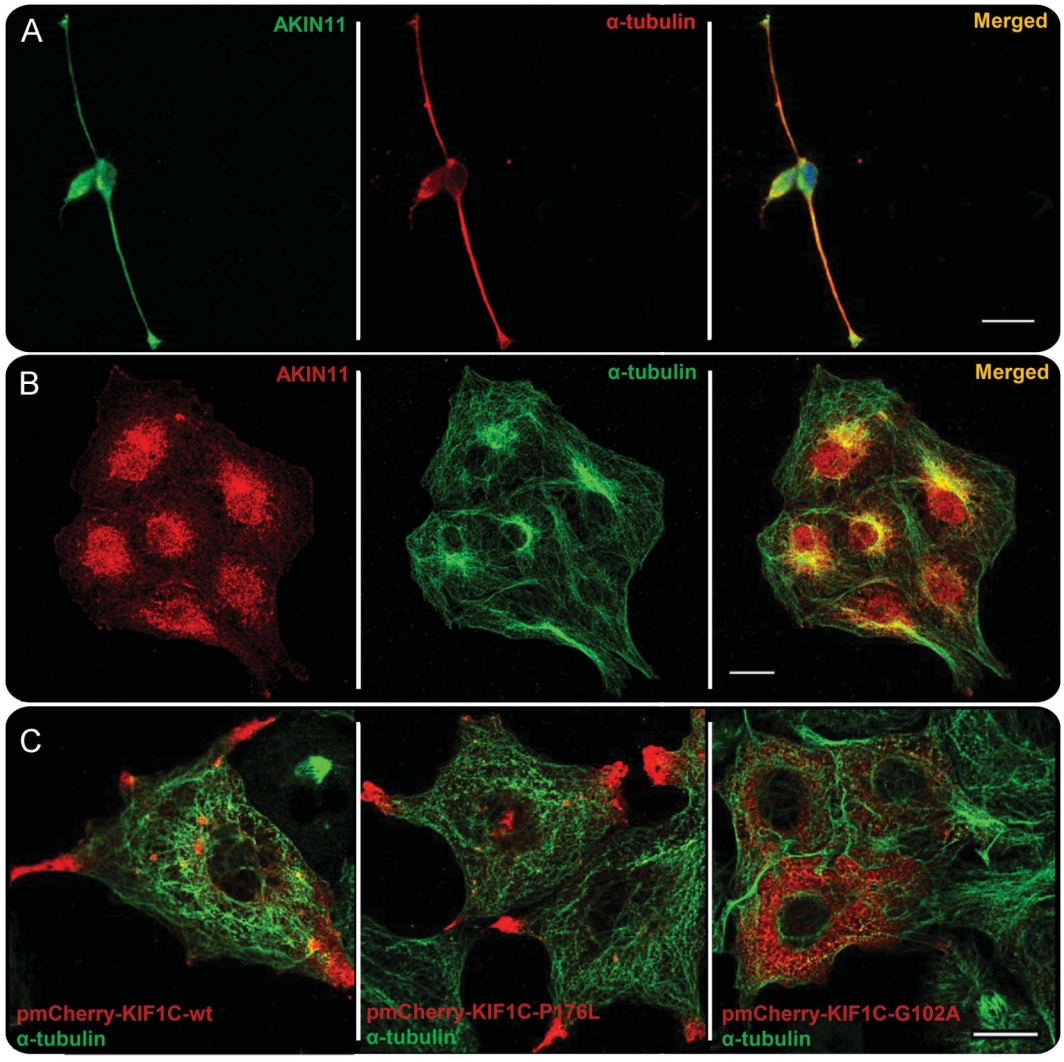

(A, B) Endogenous KIF1C. In the mouse motor neuron–like spinal cord cell line NSC-34, endogenous KIF1C is found throughout the cell body with an accumulation in the pericentrosome and along the neurites, and strong accumulation at the neurite tips (A). In fibroblast-like COS-7 cells, endogenous KIF1C is sparsely distributed throughout the cell and accumulates perinuclear in a reticular pattern (B). In COS-7 cells displaying cellular processes, accumulation at the tips of these processes can be seen (not shown). (C) Overexpressed, mCherry-tagged KIF1C accumulates at the tips of cellular processes in the COS-7 monkey fibroblast cell line (left). The same localization pattern can be observed for mCherry-tagged KIF1C-$_{Pro176Leu}$ (middle). In contrast, mCherry-tagged KIF1C$_{Gly102Ala}$ (right) fails to reach cellular processes and instead is observed in a reticular pattern around the nucleus. 200-μm scale bar.

neuroblastoma cell line (SH-SY5Y, data not shown), and a mouse spinal cord motor neuron cell line (NSC-34). As described in the literature,[7,11,12] KIF1C was located mainly in the perinuclear area with an accumulation in the pericentrosomal region. In cells forming cellular processes, i.e., NSC-34 cells or a subset of COS-7 cells, KIF1C was additionally localized along cellular processes and enriched at their tips (figure 3, A and B).

Subcellular localization of overexpressed wild-type and mutant KIF1C protein. Similarly, we found overexpressed wild-type KIF1C (pmCherry-KIF1C$_{wt}$) in the perinuclear region and strongly accumulating in the cellular processes of COS-7 cells (figure 3C). Overexpressed KIF1C$_{Pro176Leu}$ (pmCherry-KIF1C$_{Pro176Leu}$) showed a localization pattern indistinguishable from wild-type. Overexpressed KIF1C$_{Gly102Ala}$ (pmCherry-KIF1C$_{Gly102Ala}$) as well as KIF1C$_{Arg301Gly}$, however, failed to reach the tips of cellular processes and instead accumulated in a reticular pattern in a wide area around the nucleus of COS-7 cells (figure 3C, data for KIF1C$_{Arg301Gly}$ not shown).

In family THI26001, severely affected subjects carry a mixture of 2 mutant alleles, whereas the very mildly affected heterozygous mutation carriers possess only one of the mutant copies in a wild-type background. Two kinesin-3 motors closely related to KIF1C have been studied in vitro, mouse KIF1A and *Caenorhabditis elegans* Unc104.[13–15] Both appear to be active in vivo as dimers. To mimic the human situation more closely, we simultaneously overexpressed each of the mutants together with wild-type and a combination of both mutants together. As expected from the mono-overexpression experiments, simultaneous overexpression of KIF1C$_{Pro176Leu}$ and KIF1C$_{wt}$ led to colocalization of both alleles in a distribution indistinguishable from wild-type (figure 4B). Of note, upon co-overexpression of KIF1C$_{Gly102Ala}$ and KIF1C$_{wt}$, the normal distribution pattern could partially be restored and both KIF1C$_{Gly102Ala}$ and KIF1C$_{wt}$ colocalized at the tips of cellular processes (figure 4C). Overexpression of KIF1C$_{Pro176Leu}$ together with KIF1C$_{Gly102Ala}$, however, failed to restore the localization at the tips of cellular processes. Moreover, KIF1C$_{Pro176Leu}$, which shows a normal localization pattern when overexpressed alone or together with KIF1C$_{wt}$, also became trapped in the reticular perinuclear localization pattern typical for the KIF1C$_{Gly102Ala}$ mutant (figure 4D).

DISCUSSION HSPs are genetically highly heterogeneous. However, despite at least 38 known HSP genes, approximately one-third of dominant and at least half of recessive cases still cannot be explained by mutations in known genes. In this study, we uncovered the genetic basis for a new subtype of HSP with autosomal dominant and recessive inheritance—termed SPG58.

Our approach exemplifies the power of exome sequencing to identify novel disease genes even in small families, especially when combined with classic segregation analysis and access to a "validation cohort" of cases with similar phenotypes. Considering the long lists of candidate genes typically generated by exome sequencing of single families, the latter is absolutely essential to gain additional evidence for the pathogenic relevance of a novel disease gene. Collection of these "exome repositories," however, can be challenging, especially for rare diseases, and requires large collaborative efforts.[3]

KIF1C belongs to the large family of kinesin motor proteins and represents the third kinesin gene involved in the pathogenesis of HSP: mutations in the kinesin heavy chain gene *KIF5A*, encoding the main neuronal motor for long-range axonal transport, cause autosomal dominant SPG10,[16,17] and mutations in *KIF1A* cause autosomal recessive SPG30.[18,19] Kinesins are a large family of microtubule-dependent motor proteins that are involved in intracellular transport and organization of the mitotic spindle. KIF1C was first identified as a binding partner of tyrosine phosphatase PTPD1 and recognized, together with KIF1A, as a member of the so-called kinesin-3/KIF1 family based on sequence homology and the presence of a forkhead-associated domain.[7] Endogenous KIF1C is localized at the pericentrosome, in the region of the Golgi apparatus,[7] and in the cell periphery with accumulation at the tips of cellular processes, colocalizing with microtubule plus-ends.[12,20] Although the precise function of KIF1C still is not clear, it has been implicated in retrograde vesicular transport between Golgi and endoplasmic reticulum,[7] maintenance and reformation of podosomes in macrophages,[20] and stabilization of trailing adhesions in migrating cells.[12] Knockdown of KIF1C in hippocampal neurons leads to defective neurite outgrowth.[11] Most known protein interactions of KIF1C require the C-terminus (figure 1C); known interaction partners comprise 14-3-3 family proteins,[21] the nonmuscle myosin II A,[20] bicaudal-D-related protein 1 (BICDR-1),[11] and kinesin binding protein KBP.[22] Notably, some of these interaction partners are themselves associated with hereditary disorders: mutations in the myosin II A *MYH9* cause sensorineural deafness, mutations in the bicaudal D homolog 2 (*BICD2*) gene, a close homolog of BICDR-1, have recently been shown to cause a spectrum of motor neuron disorders including HSP,[23] and KBP mutations are responsible for autosomal recessive Shprintzen-Goldberg syndrome.

The 3 mutations we describe in this study are all located within the highly conserved KIF1C motor domain. The p-loop mutation Gly102Ala affects the ATP binding site of the motor. Mutations of this amino acid in KIF1A and other kinesins have been shown to impair ATP hydrolysis, lead to "rigor" binding of the immobilized motor on microtubules,[24,25] and

Figure 4 Double overexpression of mCherry- and GFP-tagged mutant and wild-type *KIF1C* alleles

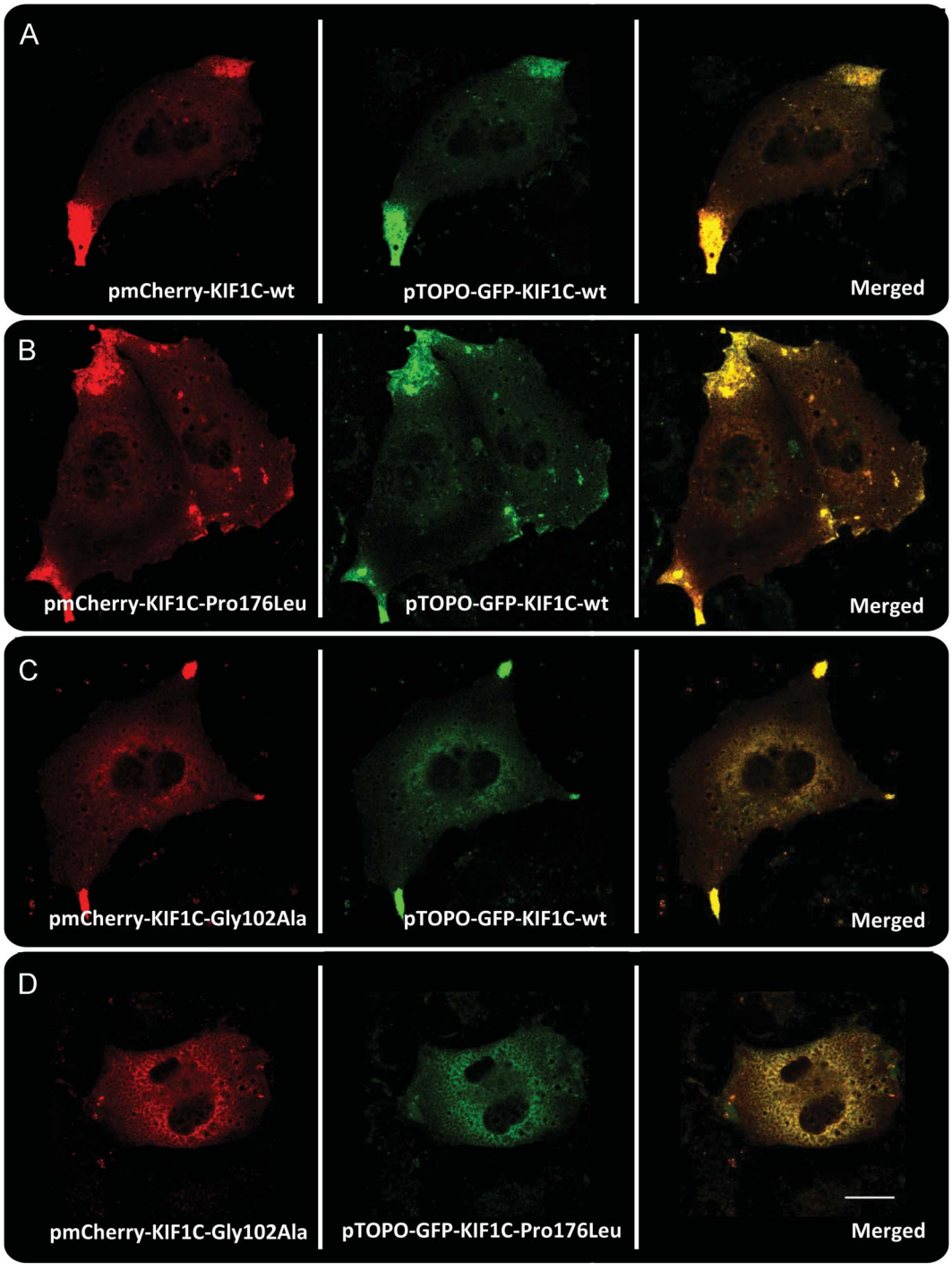

In double transfections of COS-7 cells with 2 wild-type alleles (A) or one Pro176Leu and one wild-type allele (B), the normal localization pattern consisting of a slight cytoplasmic staining combined with accumulation in cellular processes can be seen. The localization defect observed in $KIF1C_{Gly102Ala}$ mono-overexpression experiments can be partially rescued by simultaneous overexpression of $KIF1C_{wt}$ (C), but not by simultaneous overexpression of $KIF1C_{Pro176Leu}$ (D). 200-μm scale bar.

have a dominant negative effect when expressed in wild-type background.[25] Similar to the Arg301Gly mutation for which we have demonstrated reduced microtubule binding affinity and consequently reduced transport rates in the corresponding amino acid in KIF5A (Arg278),[10] the position of the Pro176Leu mutation suggests a microtubule binding defect.

While overexpression of wild-type KIF1C can rescue the perinuclear mislocalization of KIF1CGly102Ala, the KIF1CPro176Leu protein does not rescue this defect, supporting the pathogenicity of both variants.

The phenotype of SPG58 is—as is typical for HSP—variable, ranging from seemingly pure HSP to a spastic ataxia phenotype with signs of widespread

demyelination in neurophysiologic examinations and T2 hyperintensities compatible with demyelination on MRI. While this report was under review, another report of *KIF1C* mutations in 2 consanguineous families of Palestinian/Moroccan origin was published.[26] The phenotype was very similar to that of our families, with an early-onset spastic ataxia, normal cognitive function, and a similar pattern of T2 hyperintensities on MRI. Cervical dystonia, neuropathy, and reduced visual acuity were variably present.

Notably, 3 of 4 heterozygous mutation carriers that were available for examination in our study expressed a mild clinical disease phenotype as well as mild MRI changes. This dual mode of inheritance with a mild dominant disease phenotype and a more severe recessive disease expression has been previously described for at least 2 HSP subtypes. In autosomal recessive SPG7, a mild carrier phenotype mimicking autosomal dominant inheritance has been described in some families.[27] While heterozygous mutations in the heat shock protein 60 gene, *HSP60*, cause autosomal dominant pure HSP,[28] homozygous *HSP60* mutations cause an early-onset fatal hypomyelinating leukodystrophy.[29] In many ways, SPG58 exemplifies the diagnostic and counseling challenge rare hereditary diseases pose: phenotypic variability that impedes pattern recognition strategies for diagnosis, a phenotype overlapping with other disorders (hereditary ataxias and spastic paraplegias), and a mode of inheritance that blurs the lines between traditional mendelian inheritance patterns.

AUTHOR CONTRIBUTIONS

Andrés Caballero Oteyza was involved in the conceptualization of the study, acquired and analyzed most of the functional data on *KIF1C* mutations, and critically revised the article. Esra Battaloğlu was involved in design and conceptualization of the study, analyzed the genetic data on family IHG25215, and critically revised the article. Levent Ocek recruited and examined family IHG25215 and participated in drafting of the article. Tobias Lindig acquired and interpreted the MRI of family THI26001and participated in drafting of the article. Jennifer Reichbauer performed sequencing and segregation analysis of variants in family THI26001 and critically revised the manuscript. Adriana Rebelo was involved in design and conceptualization of the study and advised on the interpretation of functional data on *KIF1C* mutations; she critically revised the article. Michael Gonzalez performed exome sequencing in both families and critically revised the manuscript. Yasar Zorlu recruited and examined family IHG25215 and critically revised the article. Burcak Ozes performed sequencing and segregation analysis of variants in family IHG25215 and critically revised the manuscript. Dagmar Timmann recruited and examined family THI26001 and critically revised the article. Benjamin Bender acquired and analyzed the MRIs of family THI26001 and critically revised the article. Günther Woehlke analyzed the position of the *KIF1C* mutations and participated in drafting of the article. Stephan Züchner was involved in design of the study and critically revised the article. Ludger Schöls was involved in design of the study and critically revised the article. Rebecca Schüle was responsible for conception and design of the study, analyzed and interpreted the exome sequencing data, supervised and coordinated the study, and drafted the article. All authors approved the final version of the manuscript to be submitted.

ACKNOWLEDGMENT

The authors thank Prof. Rainer Lammers, University of Tübingen, for kindly providing the *KIF1C* cDNA.

STUDY FUNDING

Supported by the Interdisciplinary Center for Clinical Research IZKF Tübingen (grant 1970-0-0 to R.S.), the European Union (PIOF-GA-2012-326681 HSP/CMT genetics to R.S. and FP7 grant NeurOmics [2012-305121] to L.S.), the NIH (grants 5R01NS072248, 1R01NS075764, and 5R01NS054132 to S.Z.), and the German HSP-Selbsthilfegruppe e.V. (grant to R.S. and L.S.).

DISCLOSURE

A. Caballero Oteyza, E. Battaloğlu, L. Ocek, T. Lindig, J. Reichbauer, A. Rebelo, M. Gonzalez, Y. Zorlu, B. Ozes, and D. Timmann report no disclosures relevant to the manuscript. B. Bender has received travel support from Bayer Vital GmbH. G. Woehlke reports no disclosures relevant to the manuscript. S. Züchner has received license fee payments from Athena Diagnostics and is funded by NIH grants 5R01NS072248, 1R01NS075764, and 5R01NS054132. L. Schöls is funded by the EU FP7 grant 2012-305121 NeurOmics and the German HSP-Selbsthilfegruppe. R. Schüle is funded by the Interdisciplinary Center for Clinical Research IZKF Tübingen (grant 1970-0-0), the EU grant PIOF-GA-2012-326681 HSP/CMT genetics, and the German HSP-Selbsthilfegruppe e.V. Go to Neurology.org for full disclosures.

Received November 25, 2013. Accepted in final form March 3, 2014.

REFERENCES

1. Schule R, Schols L. Genetics of hereditary spastic paraplegias. Semin Neurol 2011;31:484–493.
2. Blackstone C. Cellular pathways of hereditary spastic paraplegia. Annu Rev Neurosci 2012;35:25–47.
3. Gonzalez MA, Acosta Lebrigio RF, Van Booven D, et al. GEnomes Management Application (GEM.app): a new software tool for large-scale collaborative genome analysis. Hum Mutat 2013;34:842–846.
4. Lammers R, Bossenmaier B, Cool DE, et al. Differential activities of protein tyrosine phosphatases in intact cells. J Biol Chem 1993;268:22456–22462.
5. Marx A, Hoenger A, Mandelkow E. Structures of kinesin motor proteins. Cell Motil Cytoskeleton 2009;66:958–966.
6. Okada Y, Hirokawa N. Mechanism of the single-headed processivity: diffusional anchoring between the K-loop of kinesin and the C terminus of tubulin. Proc Natl Acad Sci USA 2000;97:640–645.
7. Dorner C, Ciossek T, Muller S, Moller PH, Ullrich A, Lammers R. Characterization of KIF1C, a new kinesin-like protein involved in vesicle transport from the Golgi apparatus to the endoplasmic reticulum. J Biol Chem 1998;273:20267–20275.
8. Fichera M, Lo Giudice M, Falco M, et al. Evidence of kinesin heavy chain (KIF5A) involvement in pure hereditary spastic paraplegia. Neurology 2004;63:1108–1110.
9. Goizet C, Boukhris A, Mundwiller E, et al. Complicated forms of autosomal dominant hereditary spastic paraplegia are frequent in SPG10. Hum Mutat 2009;30:E376–E385.
10. Ebbing B, Mann K, Starosta A, et al. Effect of spastic paraplegia mutations in KIF5A kinesin on transport activity. Hum Mol Genet 2008;17:1245–1252.
11. Schlager MA, Kapitein LC, Grigoriev I, et al. Pericentrosomal targeting of Rab6 secretory vesicles by bicaudal-D-related protein 1 (BICDR-1) regulates neuritogenesis. EMBO J 2010;29:1637–1651.
12. Theisen U, Straube E, Straube A. Directional persistence of migrating cells requires Kif1C-mediated stabilization of trailing adhesions. Dev Cell 2012;23:1153–1166.
13. Hirokawa N, Nitta R, Okada Y. The mechanisms of kinesin motor motility: lessons from the monomeric motor KIF1A. Nat Rev Mol Cell Biol 2009;10:877–884.

14. Klopfenstein DR, Tomishige M, Stuurman N, Vale RD. Role of phosphatidylinositol(4,5)bisphosphate organization in membrane transport by the Unc104 kinesin motor. Cell 2002;109:347–358.
15. Yue Y, Sheng Y, Zhang HN, et al. The CC1-FHA dimer is essential for KIF1A-mediated axonal transport of synaptic vesicles in C. elegans. Biochem Biophys Res Commun 2013; 435:441–446.
16. Reid E, Kloos M, Ashley-Koch A, et al. A kinesin heavy chain (KIF5A) mutation in hereditary spastic paraplegia (SPG10). Am J Hum Genet 2002;71:1189–1194.
17. Schule R, Kremer BP, Kassubek J, et al. SPG10 is a rare cause of spastic paraplegia in European families. J Neurol Neurosurg Psychiatry 2008;79:584–587.
18. Erlich Y, Edvardson S, Hodges E, et al. Exome sequencing and disease-network analysis of a single family implicate a mutation in KIF1A in hereditary spastic paraparesis. Genome Res 2011;21:658–664.
19. Klebe S, Lossos A, Azzedine H, et al. KIF1A missense mutations in SPG30, an autosomal recessive spastic paraplegia: distinct phenotypes according to the nature of the mutations. Eur J Hum Genet 2012;20:645–649.
20. Kopp P, Lammers R, Aepfelbacher M, et al. The kinesin KIF1C and microtubule plus ends regulate podosome dynamics in macrophages. Mol Biol Cell 2006;17:2811–2823.
21. Dorner C, Ullrich A, Haring HU, Lammers R. The kinesin-like motor protein KIF1C occurs in intact cells as a dimer and associates with proteins of the 14-3-3 family. J Biol Chem 1999;274:33654–33660.
22. Wozniak MJ, Melzer M, Dorner C, Haring HU, Lammers R. The novel protein KBP regulates mitochondria localization by interaction with a kinesin-like protein. BMC Cell Biol 2005;6:35.
23. Oates EC, Rossor AM, Hafezparast M, et al. Mutations in BICD2 cause dominant congenital spinal muscular atrophy and hereditary spastic paraplegia. Am J Hum Genet 2013;92:965–973.
24. Meluh PB, Rose MD. KAR3, a kinesin-related gene required for yeast nuclear fusion. Cell 1990;60:1029–1041.
25. Wedlich-Soldner R, Straube A, Friedrich MW, Steinberg G. A balance of KIF1A-like kinesin and dynein organizes early endosomes in the fungus Ustilago maydis. EMBO J 2002;21: 2946–2957.
26. Dor T, Cinnamon Y, Raymond L, et al. KIF1C mutations in two families with hereditary spastic paraparesis and cerebellar dysfunction. J Med Genet 2013;51:137–142.
27. Klebe S, Depienne C, Gerber S, et al. Spastic paraplegia gene 7 in patients with spasticity and/or optic neuropathy. Brain 2012;135:2980–2993.
28. Hansen JJ, Durr A, Cournu-Rebeix I, et al. Hereditary spastic paraplegia SPG13 is associated with a mutation in the gene encoding the mitochondrial chaperonin Hsp60. Am J Hum Genet 2002;70:1328–1332.
29. Magen D, Georgopoulos C, Bross P, et al. Mitochondrial hsp60 chaperonopathy causes an autosomal-recessive neurodegenerative disorder linked to brain hypomyelination and leukodystrophy. Am J Hum Genet 2008;83:30–42.